Supporting Information

Ghosh *et al.* 10.1073/pnas.0803182105

SI Materials and Methods

Materials. Two p38 MAP kinase inhibitors, 2-(4-chlorophenyl)-4-(4-fluorophenyl)-5-pyridin-4-yl-1,2-dihydropyrazol-3-one (CFPD) and SB202190, a MEK1/2 inhibitor PD98059, and two proteasome inhibitors (MG132 and lactacystin), were procured from Calbiochem. TNFα was from Invitrogen; tissue culture grade H_2O_2 and other chemicals were from Sigma. Human IFN α (HuIFNα2A) was obtained from PBL IFN Source. Mouse monoclonal PCBP2 antibody was from Novus Biological, and the SIN1 antibody used for immunofluorescence was a rabbit antiserum prepared against ovine SIN1 from a GST fusion protein prepared in this laboratory (1). A later preparation was made with the same fusion protein by Proteintech and was used for Western blotting and immunoprecipitation. Affinity-purified antibodies to phosphorylated MEK1/2 (Ser-217/221) and phosphorylated p38 MAP kinase (Thr-180/Tyr-182) were obtained from Cell Signaling Technology. Rabbit polyclonal antibodies for TNFR1 and TNFR2 were from Novus Biologicals and Cell Signaling Technology, respectively. The rabbit polyclonal antibody to type I IFN receptor 2 (IFNAR2) was purchased from Abcam (Cambridge, MA). All of the antibodies were used at a dilution of 1:2000.

Yeast Two-Hybrid Screen. Yeast (*S. cerevisiae*) cell lines AH109 and Y187 and the human bone marrow library (BD Matchmaker pretransformed library) were obtained from BD Clontech. A full length SIN1 cDNA (1,676 bp encoding 522 aa) was amplified by using full-length SIN1F and Full length SIN1R primers (Table S4) with EcoRI and SalI restriction site linkers and subcloned into the pGBKT7 vector, which was transformed into yeast strain AH109. After transformation, yeast cells were plated onto glucose-based SD agar plates lacking Trp (SD/_Trp), on which only transformed cells are able to grow. Basal activation of the SIN1 bait was determined by measuring the growth rate in SD/_Trp-Leu-His-Ade medium and toxicity of bait protein by culturing in SD/_Trp medium. The human bone marrow library, pretransformed into Y187 yeast, was mixed with a concentrated culture of AH109 in YPDA medium. The mixed yeast culture was maintained at 30°C at 30 rpm for 24–30 h and then plated on SD/_Trp-Leu-His-Ade plate containing kanamycin and 15 mM 3-aminotriazole (3-AT). Yeast colonies bigger than 2 mm in diameter were picked for further analysis.

Yeast plasmid isolation and PCR: Based on strength of reporter gene expression, yeast colonies were selected for plasmid isolation following the procedure provided by Zymo Research. DNA was precipitated with isopropanol, dried, dissolved in TE buffer, amplified by PCR, and sequenced. The presence of bait plasmid in the selected interacting clones was verified by PCR with pGBKT7 bait vector specific primers (pGBKT7F and pGBKT7R) (Table S4).

Reporter Gene Expression. In response to GAL4 activation, AH109 and Y187 yeast cells secrete β-galactosidase whose activity from overnight cultures was assayed by using reagents from Pierce. Values were normalized relative to control culture medium and cell density.

In response to GAL4 activation, AH109 and Y187 yeast cells secrete α-galactosidase (product of *MEL 1*), which can be detected on a solid plate containing the substrate X-α-Gal (Clontech). A stock solution of X-α-Gal (2 mg/ml dimethyl formamide) was used undiluted to coat SD/_Trp-Leu-Ade-His plates and allowed to air-dry. Yeast recombinants were streaked on the plate and incubated at 30°C. The intensity of the blue color was used to assess the strength of the interaction between the SIN1 bait and the interacting protein encoded by the pGADT7 activation domain (AD) vector.

GST Pull-Down Assay. The SIN1 constructs described above were subcloned into pGEX-4T-1 by using the same primers and same restriction site linkers as used to subclone into the pGBKT7 vector. GST fusion proteins were prepared (2), and 10 μg of each incubated overnight with HeLa cell extracts containing 0.2 mg protein in "binding" buffer. Complexes were collected on glutathione-Sepharose beads (GE Healthcare BioSciences). After washing, protein complexes were eluted from the beads and analyzed by SDS/PAGE and Western blotting (3) with either an affinity purified polyclonal antibody against SIN1 or a mouse monoclonal antibody against PCBP2, both diluted 1:2,000.

Coimmunoprecipitations. Interactions between SIN1 and PCBP2 were assayed by coimmunoprecipitation. Coimmunoprecipitations were also used to assess the interaction of SIN1 and PCBP2 with TNFα and IFN receptors in the presence or absence of 1000 units/ml HuIFNα2A or 50 ng/ml TNFα for 6 h.

All coimmunoprecipitations were performed by standard procedures (4). Briefly 500 μg and 1 mg of HeLa cell extract were precleared and incubated with specific antibodies for overnight. Preswollen, washed protein G beads (Santa Cruz Biotechnology) were added to cell extract preincubated with specific antibody and incubated further for 6 h. The beads were washed five times and coimmunoprecipitated protein complexes were eluted and analyzed by SDS/PAGE and reciprocal Western blotting (3).

Western Blotting. Western blotting was performed to measure SIN1 and PCBP2 protein concentrations by using specific antibodies after addition of TNFα, H_2O_2, MG132, or protein kinase inhibitors. The relative intensities of bands on blots were measured by densitometric scanning and analyzed with NIH ImageJ software.

TUNEL Staining and Estimation of Apoptosis. Cells were grown on Lab-Tek chamber slides (Electron Microscopy Sciences), transfected with 40 nM siRNAs (Table S2), and cultured for a further 72 h. At this stage, cells were exposed to either 10 ng/ml and 50 ng/ml TNFα (Invitrogen) or 50 μM and 100 μM H_2O_2. After 6 h, cells were fixed in 4% paraformaldehyde and apoptotic nuclei identified by using the DeadEnd Fluorometric TUNEL System from Promega. Nuclei were counterstained with propidium iodide, and cells photographed under epifluorescent optics. Two-color images of a minimum of three randomly chosen fields from each image ($\times$40 magnification) were prepared for each treatment, and the number of apoptotic cells calculated as a percentage of total cells by using Photoshop CS3 version 8.0.

To assess the effect of protease inhibitor MG132 on cell phenotype and cell death, HeLa cells were either left untreated or treated with 10 μM MG132 for 4, 6, and 8 h and TUNEL-stained. A similar experiment was performed to measure cell viability after treating with MG132 by Trypan blue exclusion. The medium from each well after treatment was removed, replaced with 0.5% Trypan blue, and incubated at 25°C for 10–15 min, and cells were examined under an inverted microscope.

Immunofluorescent Localization of Antigens. HeLa cells (2×10^5 cells per well) were plated on sterile cover slips in 1 ml of medium in individual wells of six-well plates. After 16 h cultures were exposed to 50 ng/ml TNFα or 100 μM H_2O_2 in culture medium for 4, 6, 10, and 20 h. Control cultures were supplied with fresh medium lacking additives. After treatment, the cells were washed, fixed (4% paraformaldehyde; 20 min), and permeabilized with 0.2% Triton X-100 for 10 min. The fixed, permeabilized cell monolayers were treated concurrently with 5% IgG-free BSA (Jackson Immunoresearch Laboratories) and 5% goat serum in PBS for 1 h, and then exposed to primary antibodies (affinity-purified rabbit anti-SIN1 and mouse anti-PCBP2, each diluted 1:500 in 5% BSA) overnight. Cells were then washed three times in PBS containing 0.1% Triton X-100 and incubated for 2h with secondary antibodies (Alexa Fluor 488 F(ab′)2, goat anti-rabbit IgG and Alexa Fluor 568 F(ab′)2 goat anti-mouse IgG (Molecular probes, Invitrogen), each diluted 1:2000. Nuclei were stained with 4′, 6-diamido-2-phenylindole hydrochloride (DAPI; 1 μg/ml; Sigma–Aldrich) in PBS at room temperature for 15 min. After additional washes with PBS, coverslips were mounted on glass slides in ProLong Gold anti-fade reagent (Molecular Probes, Invitrogen). The photographs from each experiment were taken on a Confocal Microscope, model Zeiss LSM 510 META.

Predicting Functional Partners for SIN1 and PCBP2. Human microarray data from NCBI Gene Expression Omnibus (www.ncbi.nlm.nih.gov/geo/) SOFT (Simple Omnibus in Text Format) were analyzed to determine the datasets in which *SIN1* and *PCBP2* showed a significant (up or down) change in expression level (5). In the second step, Meta Analysis (6) was performed on these datasets to determine which genes were coexpressed with *SIN1*. The analysis created a statistical neighboring linkage graph based on their functional similarity score (in this case χ^2 metastatistics), and its significance level (7). Close neighbors, i.e., genes that significantly shifted their expression levels in the same direction as the gene under study, e.g., *SIN1*, over time or in response to treatments, for example, were assumed to be related in function. Here the metaanalysis was confined to a single dataset microarray platform, GPL96, i.e., an Affymetrix GeneChip Human Genome U133 Array Set HG-U133A and used 13 curated microarray datasets, each of which had between 50 arrays and 154 arrays (Table S3). First, the data were preprocessed and analyzed separately to provide two separate neighbor lists for SIN1 and PCBP2, respectively. The genes in common to each list with a significance level of $P < 0.01$ were then identified and ranked, based on associated confidence scores. The annotations of these identified genes were used to predict potential functions of *SIN1* and *PCBP2*.

1. Wang SZ, Roberts RM (2004) Interaction of stress-activated protein kinase-interacting protein-1 with the interferon receptor subunit IFNAR2 in uterine endometrium. *Endocrinology* 145:5820–5831.
2. Volkel D, Blankenfeldt W, Schomburg D (1998) Large-scale production, purification and refolding of the full-length cellular prion protein from Syrian golden hamster in Escherichia coli using the glutathione S-transferase-fusion system. *Eur J Biochem* 251:462–471.
3. Ghosh D, Ezashi T, Ostrowski MC, Roberts RM (2003) A central role for Ets-2 in the transcriptional regulation and cyclic adenosine 5′-monophosphate responsiveness of the human chorionic gonadotropin-beta subunit gene. *Mol Endocrinol* 17:11–26.
4. Ghosh D, Sachdev S, Hannink M, Roberts RM (2005) Coordinate regulation of basal and cyclic 5′-adenosine monophosphate (cAMP)-activated expression of human chorionic gonadotropin-alpha by Ets-2 and cAMP-responsive element binding protein. *Mol Endocrinol* 19:1049–1066.
5. Lee HK, Hsu AK, Sajdak J, Qin J, Pavlidis P (2004) Coexpression analysis of human genes across many microarray data sets. *Genome Res* 14:1085–1094.
6. Hedges L, Olkin I (1985) *Statistical Methods for Meta-Analysis* (Academic, New York).
7. Chen Y, Xu D (2004) Global protein function annotation through mining genome-scale data in yeast Saccharomyces cerevisiae. *Nucleic Acids Res* 32:6414–6424.

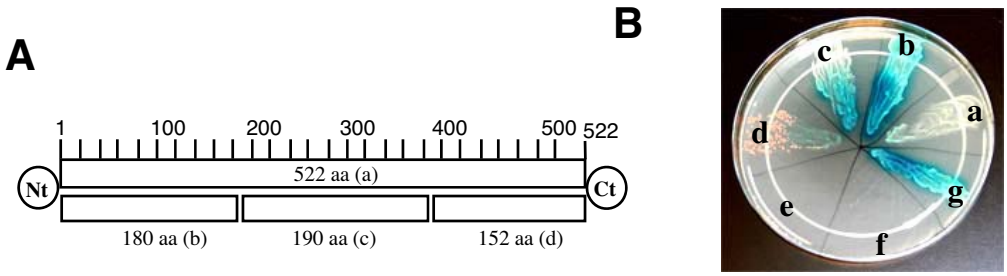

Fig. S1. Yeast two-hybrid analysis of the interaction between SIN1 and PCBP2. (*A*) Schematic representation of the highly conserved SIN1 protein, which is predicted to be 522 aa. Three truncated SIN1 constructs, N-terminal 180 aa (b), central region of 190 aa (c), and the C-terminal 152 aa (d) were used as the bait in the AH109 yeast strain. (*B*) Confirmation of SIN1 and PCBP2 interactions shown by β-galactosidase activity in Fig. 1*A*. The yeast was plated on SD/_Trp-Leu-Ade-His plates with X-alpha Gal as substrate to assess MEL1 activation. AH109 strain transformed with pGBKT7–53 (bait vector) and Y187 transformed with pGADT7-T were used as the positive control (g). The growth and α-galactosidase activities (blue) are shown for the b, c, and d bait constructs and for a full-length SIN1 (a). AH109 strain transformed with the full-length SIN1 bait only (e) and Y187 with PCBP2 in the activation domain vector only (f) were the negative controls.

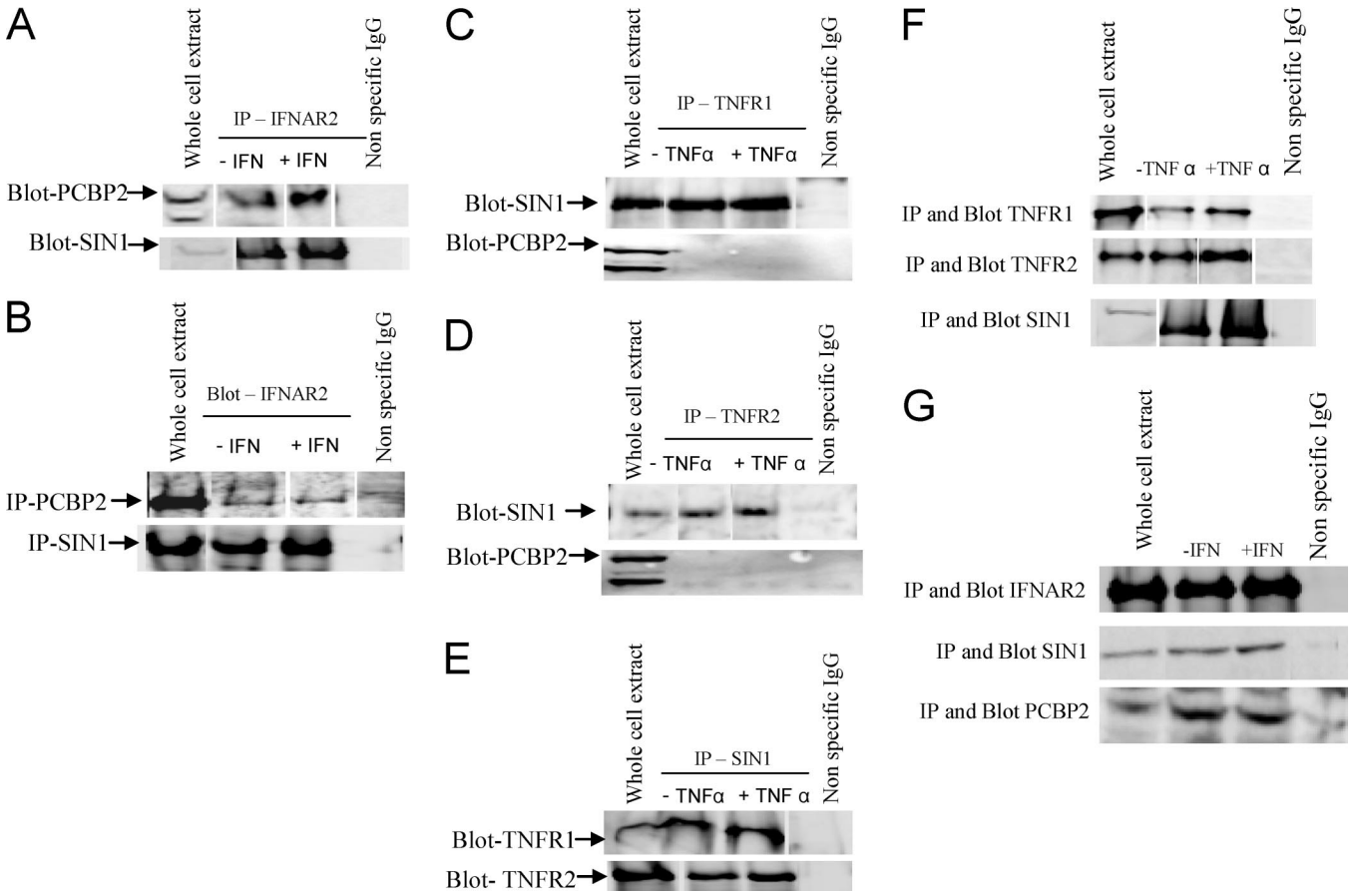

Fig. S2. Experiments designed to illustrate the interaction of SIN1 and PCBP2 with the type I IFN receptor subunit, IFNAR2 (*A* and *B*) and with the TNFα receptor subunits TNFR1 and TNFR2 (*C*–*E*). (*A*) HeLa cells were either left untreated or were treated with 1,000 units/ml human IFNα2A for 6 h. Whole-cell lysates were immunoprecipitated with IFNAR2 antibody, and detection of antigens on Western blots was done by using either PCBP2 or SIN1 antibodies. (*B*) Similar to *A* except immunoprecipitations were performed with either anti-PCBP2 or anti-SIN1 and Western blots developed by using anti-IFNAR2. (*C* and *D*) HeLa cells were either left untreated or were treated with 50 ng/ml TNFα for 6 h. Complexes were immunoprecipitated with either anti-TNFR1 (*C*) or anti-TNFR2 (*D*), and Western blots were developed by using either SIN1 or PCBP2 antibodies. (*E*) As in *D*, except immunoprecipitations were performed with anti-SIN1 and Western blots developed with anti-TNFR1 and TNFR2. (*F*) To verify efficiency of antigen immunoprecipitation, immunoprecipitations and Western blotting were performed with the same antibodies, anti-TNFR1 (*Top*), or anti-TNFR2 (*Middle*), or anti-SIN1 (*Bottom*). The experiments were conducted in the presence or absence of 50 ng/ml TNFα for 6 h. (*G*) immunoprecipitations and Western blotting were performed with the same antibodies, anti-IFNAR2 (*Top*), anti-SIN1 (*Middle*), or anti-PCBP2 (*Bottom*). The experiments were conducted in the presence or absence of 1,000 unts/ml human IFNα2A for 6 h. The white ''gaps'' between some of the images indicate where irrelevant lanes have been omitted to construct the figures.

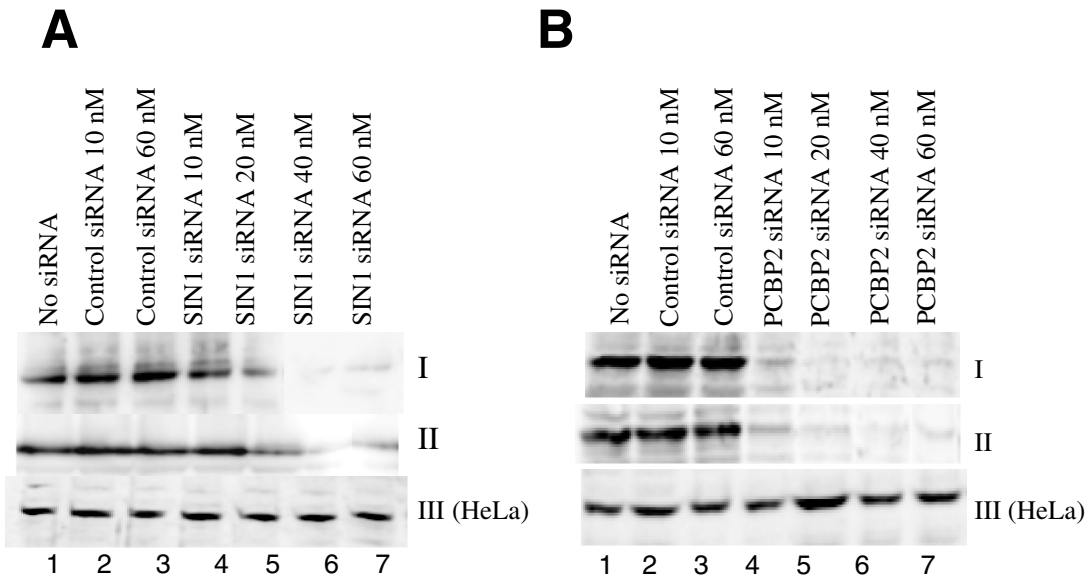

Fig. S3. Western blot analysis of HeLa and 3T3 cell extracts after knockdown of SIN1 (*A*) and PCBP2 (*B*) by siRNA transfection. (*A*) HeLa cells (I) and NIH 3T3 fibroblasts (II) were transfected with increasing concentrations (10 nM, 20 nM, 40 nM, and 60 nM) of a gene-specific SIN1 siRNA (lanes 4–7) and a nonspecific siRNA (10 nM and 60 nM) (lanes 2 and 3). Cell lysates (100 μg of protein per lane) were analyzed by SDS/PAGE, and Western blotting was performed with anti-SIN1 as the detecting reagent. Relative SIN1 concentrations in untreated cells are represented in lane 1. III is a Western blot identical to that in I but immunostained for β-actin. (*B*) HeLa cells (I) and NIH 3T3 fibroblasts (II) were transfected with increasing concentrations (10 nM, 20 nM, 40 nM, and 60 nM) of a PCBP2 siRNA (lanes 4–7) and a nonspecific siRNA (10 nM and 60 nM) (lanes 2 and 3). The Western blot analysis was identical to that in *A* except the detecting antibody was anti-PCBP2. III is a Western blot identical to that in I but immunostained for β-actin. The white ''gaps'' between some of the images indicate where irrelevant lanes have been omitted to construct the figure.

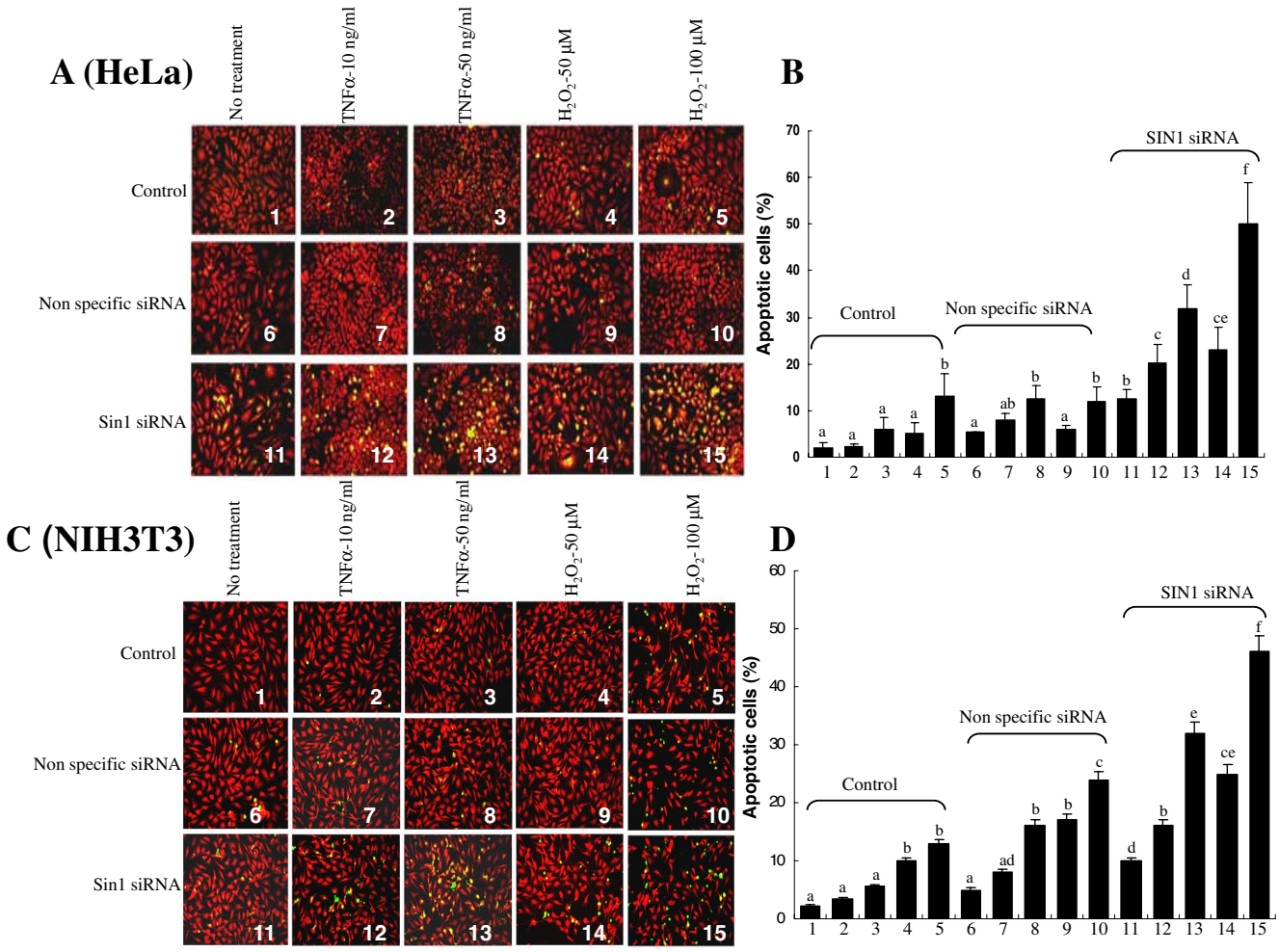

Fig. S4. Apoptosis detected by TUNEL staining in response to cellular stress after siRNA silencing of SIN1 in HeLa and NIH 3T3 fibroblasts. (*A*) HeLa cells were transfected with either 40 nM of a nonspecific control siRNA (middle row) or 40 nM of a SIN1 siRNA (third row) and cultured for a further 72 h. The upper row represents nontransfected cells. At 72 h, the monolayers were exposed to TNFα (10 ng/ml and 50 ng/ml) and H_2O_2 (50 μM and 100 μM) and cultured a further 6 h before fixation, TUNEL staining (to show nuclei from cells undergoing apoptosis, green), and counterstaining with propidium iodide (shown in red). The figure is composed entirely of merged epifluorescence images. Costaining appears yellow. (*B*) The percentage of apoptotic cells expressed as a percentage of total cells. Bars 1, 6, and 11 represent the number of apoptotic cells in cultures not exposed to cell stressor; bars 2, 7, and 12 and bars 3, 8, and 13 are values from cultures treated with either 10 ng/ml or 50 ng/ml TNFα, respectively; bars 4, 9, and 14 and bars 5, 10, and 15 are values from cultures treated with either 50 μM or 100 μM H_2O_2, respectively. Results are shown as mean percentage of apoptotic cells $\pm$ SEM from five independent experiments, with a minimum of three fields of $>$300 cells counted in each. Where letters differ above bars within individual treatments, values are significantly different ($P < 0.05$). (*C*) The effect of SIN1 silencing on apoptosis in 3T3 cells. The experiment was identical to that in *A*, except 3T3 rather than HeLa cells were used. (*D*) Same as *B* except 3T3 rather than HeLa cells were used.

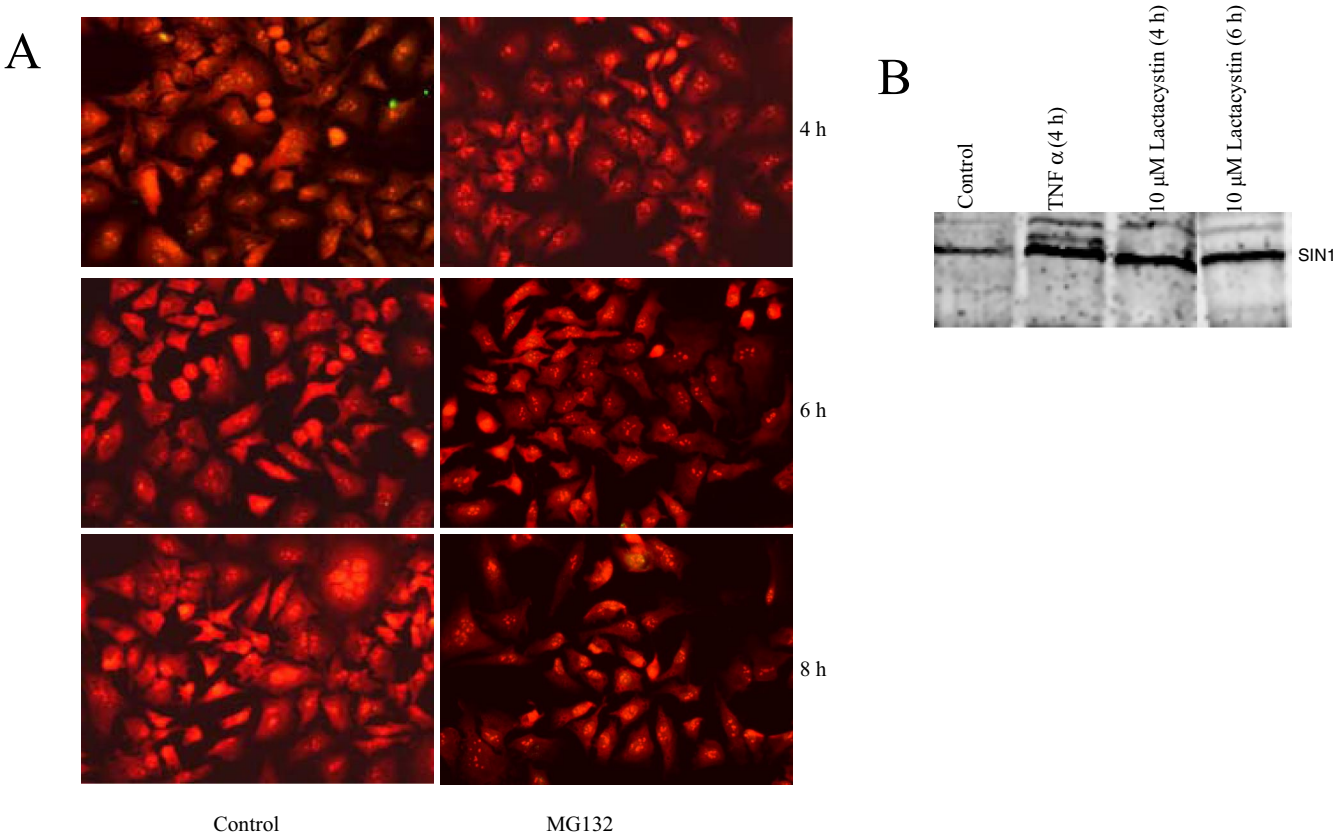

Fig. S5. (*A*) Assessment of MG132 toxicity on HeLa cells. Cells were treated with 10 μM MG132 for 4, 6, and 8 h, and apoptotic nuclei were identified by TUNEL staining. (*B*) A comparison of the effects of TNFα (50 ng/ml, 4 h) and treatment with the proteasome inhibitor lactacystin (10 μM; 4 h, lane 3; 6 h, lane 4) on the SIN1 concentration of HeLa cells. Western blotting was performed by using anti-SIN1.

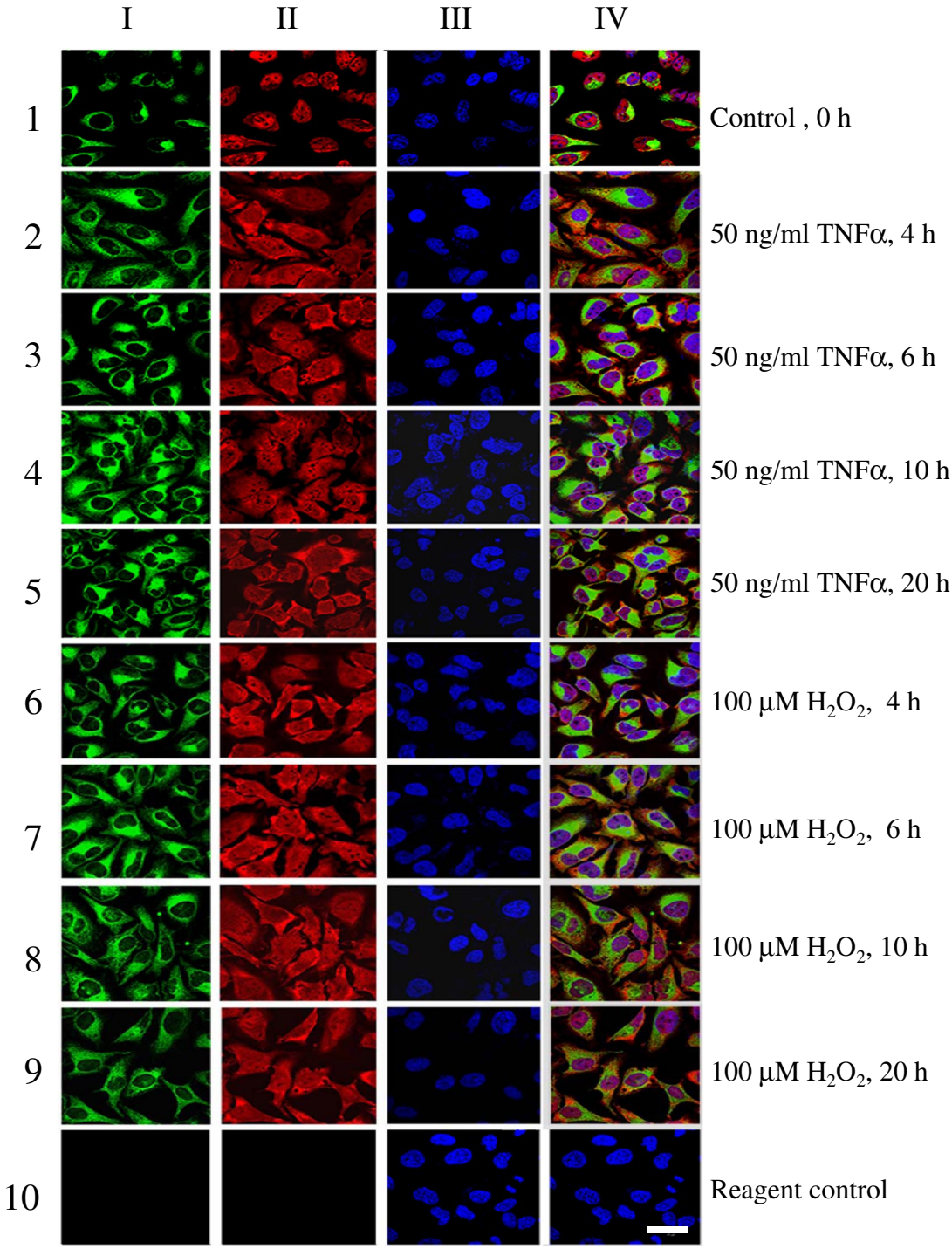

Fig. S6. Localization of SIN1 (green) and PCBP2 (red) in HeLa cells by immunofluorescence after treatments with TNFα and H_2O_2. HeLa cells were treated with either 50 ng/ml TNFα or 100 μM H_2O_2 for 4 h, 6 h, 10 h, and 20 h. Untreated controls were examined at each time point but are shown only for 0 h (1), because no changes in SIN1 and PCBP2 localization were observed at subsequent time points. Cells were fixed and immunostained for either SIN1 (I) or PCBP2 (II) and counterstained with DAPI (III). Merged images are shown in IV. A reagent control that used a nonspecific IgG as primary antibody is also shown in row 10. (Scale bar: 20 μm.)

Table S1. Potential interacting proteins obtained in the yeast two-hybrid screen human bone marrow library with SIN1 as bait

Protein	GenBank accession ID	No. of clones
Human ribosomal protein S20 (RPS20)	AK130961 and NP_001014	11
Human cDNA	FLJ34729 (unknown protein)	6
Human poly(rC)binding protein 2 (PCBP2)	AK123458	7
Human polyglutamine binding protein variant 4 (PQBP1)	AJ97396	7
Human hemoglobin α2 (HBA2)	NM_00517	5
Human WAS protein family member 2 (WAVE2/WASF2)	AL66122	6
Human defensin α1 (DEFA1)	NM_004084 and XM_928349	4
Human TGFβ-induced apoptosis protein 2 (TAIP2)	AB063300	2
Human TNNI3-interacting kinase (TNNI3K)	CAE45949	1

Table S2. Short siRNA sequences used to knock down *SIN1* and *PCBP2*

Primer name	Sequence	
	Sense	Antisense
130550	5′-GCAGUCGAUAUUAUCUGUAtt-3′	5′-UACAGAUAAUAUCGACUGCtt-3′
30914	5′-GGAGUUAAAGUCACUGUUUtt-3′	5′-AAACAGUGACUUUAACUCCtg-3′
284822	5′-GCGAAGAAAAGGAUCCCAGtt-3′	5′-CUGGGAUCCUUUUCUUCGCtt-3′
143967	5′-GGCCUAUACCAUUCAAGGAtt-3′	5′-UCCUUGAAUGGUAUAGGCCtc-3′
143966	5′-CCUCUAGAGGCCUAUACCAtt-3′	5′-UGGUAUAGGCCUCUAGAGGtg-3′

130550, 30914, and 284822, predesigned siRNAs to silence *SIN1* gene expression, and 143967 and 143966, predesigned siRNA targeted to PCBP2 transcripts, were purchased from Ambion.

Table S3. Microarray data set information

Series number/no. of arrays	Accession ID	Data set description
1/158	GDS1064.soft	Expression profiling of bone marrow from 43 patients with various forms of acute myeloid leukemia (AML).
2/127	GDS1209.soft	Expression profiling of soft tissue sarcoma samples. Hypoxic regions often develop in tumors as they increase in size. Results provide insight into the expression of hypoxia-related genes in sarcomas.
3/87	GDS1220.soft	Expression profiling of malignant pleural mesothelioma (MPM) tumors. MPM is a highly lethal malignancy associated with asbestos exposure. Results provide insight into the pathogenesis of MPM.
4/85	GDS1375.soft	Expression profiling of primary malignant melanoma, benign skin nevi, and normal skin samples. Results identify potential molecular markers for lymph node staging assays and provide insight into melanoma tumorigenesis.
5/76	GDS1428.soft	Analysis of neutrophils at various time points up to 24 h after infection with *Anaplasma phagocytophilum*, an obligate intracellular bacterium. *A. phagocytophilum*, the agent of granulocytic anaplasmosis, avoids destruction by delaying neutrophil apoptosis.
6/75	GDS1479.soft	Analysis of bladder biopsies of superficial transitional cell carcinomas with or without surrounding carcinoma *in situ* (CIS) lesions and muscle-invasive carcinomas (mTCC). CIS is a common mTCC precursor. Results provide insight into which tumors in early-stage bladder cancer are likely to progress.
7/70	GDS1615.soft	Analysis of peripheral blood mononuclear cells (PBMCs) from Crohn's disease (CD) and ulcerative colitis (UC) patients. Results identify a PBMC expression signature that distinguishes between CD and UC, suggesting that diagnosis of these two inflammatory bowel diseases (IBD) using PBMCs is possible.
8/67	GDS1975.soft	Analysis of grade III and grade IV gliomas of various histologic types. Results are used to develop a gene-expression-based, histology-independent classification scheme and provide insight into the biology of gliomas.
9/61	GDS2113.soft	Analysis of 76 adrenal and extraadrenal pheochromocytomas. These neural crest-derived tumors of uniform phenotype arise from inherited or sporadic mutations in at least six independent genes. Results provide insight into the molecular pathogenesis of pheochromocytomas.
10/60	GDS2190.soft	Analysis of postmortem dorsolateral prefrontal cortex from 30 adults with bipolar disorder. Results provide insight into the pathophysiology of the disease.
11/54	GDS534.soft	Analysis of cigarette-smoking-induced changes in bronchial epithelia and reversibility of effects when smoking is discontinued. May provide insight into molecular events leading to chronic obstructive pulmonary disease (COPD) and lung cancer.
12/54	GDS596.soft	Gene atlas of human protein-encoding transcriptome. Examined gene expression profiles from 79 physiologically normal tissues obtained from various sources.
13/52	GDS715.soft	Expression profiling of HL-60 and acute promyelocytic leukemia cells treated with various drugs. Results identify drugs that produce profiles consistent with differentiation of AML cells and thus are candidates for treating AML.

Shown is the list of data sets downloaded from the National Center for Biotechnology Information Gene Expression Omnibus and used for meta analysis. Each of these data sets has at least 50 columns (arrays).

Table S4. Synthetic oligonucleotides used for subcloning and PCR

Primer name	Sequence
Full-length SIN1 sense	5′-GCA TGA ATT CAT GGG CTT CTT GGA CAA TCC AAC-3′
Full-length SIN1 antisense	5′-CCA AGT CGA CTC ACT GCT GCC CTG ATT TCT TTT C-3′
Nt-SIN1 sense	5′-TGG TGC CTG AAT TCA TGG GCT TCT TGG ACA ATC-3′
Nt-SIN1 antisense	5′-GAA TTT AAG TCG ACT CGG CAG CAG TCT GTC C-3′
Mh-SIN1 sense	5′-GAA TCG CTG AAT TCA TGA CGG TGG TGA CTA TGG-3′
Mh-SIN1 antisense	5′-CAT CGC CAG TCG ACG CTG ACT TTG AAT GAC T-3′
Ct-SIN1 sense	5′-GCT AGG CAG AAT TCA TGA TCC ACA GAC TCC GCT T-3′
Ct-SIN1 antisense	5′-ATA CCC AAG TCG ACT CAC TGC TGC CCT GAT TTC T-3′
M13F	5′-CGT TGT AAA ACG ACG GCC AGT-3′
M13R	5′-CAG GAA ACA GCT ATG ACC ATG-3′
pGADT7F	5′-CTA TTC GAT GAT GAA GAT ACC CCA CCA AAC CC-3′
pGADT7R	5′-GTG AAC TTG CGG GGT TTT TCA GTA TCT ACG ATT-3′
pGBKT7F	5′-TCA TCG GAA GAG AGT AGT-3′
pGBKT7R	5′-AGA GTC ACT TTA AAA TTT GTA TAC-3′
pGEX-4TF	5′-CCA GCA AGT ATA TAG CAT GG-3′
pGEX-4TR	5′-CCG GGA GCT GCA TGT GTC AGA GG-3′
SIN1-F1	5′-CCA GTC GGT CGA TAT TAC CT-3′
SIN1-R2	5′-GTG TTG TCC ACC TGG ATA AG-3′
SIN1-R3	5′-TGC TCG CGA TTC CAG TAT GT-3′
RPL7F	5′-TCA ATG GAG TAA GCC CAA AG-3′
RPL7R	5′-CAA GAG ACC GAG CAA TCA A

Other Supporting Information Files

Dataset S1 (XLS)
Dataset S2 (XLS)
Dataset S3 (XLS)